

## Article

# Seven New Lobane Diterpenoids from the Soft Coral *Lobophytum catalai*

Jiarui Zhang<sup>1,2</sup>, Huixue Ma<sup>1,2</sup>, Shuangshuang Jin<sup>1,2</sup>, Xuehuan Liu<sup>1,2</sup>, Lei Li<sup>3</sup>, Zhaonan Liu<sup>1,2</sup>, Guoqiang Li<sup>1,2,\*</sup>  and Pinglin Li<sup>1,2,\*</sup>

- <sup>1</sup> Key Laboratory of Marine Drugs, Chinese Ministry of Education, School of Medicine and Pharmacy, Ocean University of China, Qingdao 266003, China
- <sup>2</sup> Laboratory of Marine Drugs and Biological Products, National Laboratory for Marine Science and Technology, Qingdao 266235, China
- <sup>3</sup> Biology Institute, Qilu University of Technology (Shandong Academy of Sciences), Jinan 250103, China
- \* Correspondence: liguoqiang@ouc.edu.cn (G.L.); lipinglin@ouc.edu.cn (P.L.); Tel.: +86-532-8203-2323 (G.L.); +86-532-8203-3054 (P.L.)

**Abstract:** Seven new lobane diterpenoids, namely, lobocatalens A–G (1–7), were isolated from the Xisha soft coral *Lobophytum catalai*. Their structures, including their absolute configurations, were elucidated via spectroscopic analysis, comparison with the literature data, QM-MNR, and TDDFT-ECD calculations. Among them, lobocatalen A (1) is a new lobane diterpenoid with an unusual ether linkage between C-14 and C-18. In addition, compound 7 showed moderate anti-inflammatory activity in the zebrafish models and cytotoxic activity against the K562 human cancer cell line.

**Keywords:** *Lobophytum catalai*; lobocatalens A–G; lobane diterpenoids; anti-inflammatory activity; cytotoxic activity

## 1. Introduction

Lobane diterpenoids are a group possessing a unique prenylated  $\beta$ -elemene carbon framework [1,2], which are seldom discovered in marine natural products. Since the first lobane diterpenoid, fuscol, was isolated from the Caribbean gorgonian coral in 1978 [3], no more than 20 lobane diterpenoids have been discovered in the last twenty years [4–9]. Nevertheless, these lobane-type diterpenoids show a wide range of biological activities such as antibacterial [10], cytotoxic [11], and anti-inflammatory activity [9], displaying impressive value worthy of further investigation.

The soft corals of the genus *Lobophytum* (family Alcyoniidae) are well known as a rich source of lobane diterpenoids [4–9], cembranolides [12–15], and prenylgermacrane-type diterpenoids [16]. With the aim of seeking new bioactive lobane diterpenoids, our continuing investigation of the soft coral *Lobophytum catalai* collected from Yagong Island led to the isolation of seven new lobane diterpenoids. Considering that there have been no reports on lobane-based diterpenoids from the soft coral *Lobophytum catalai*, these new compounds, 1–7, were named lobocatalens A–G (Figure 1). Among them, lobocatalen A (1) is a new lobane diterpenoid with an unusual ether linkage between C-14 and C-18. In addition, compound 7 showed moderate anti-inflammatory activity in the zebrafish models and moderate cytotoxic activity against the K562 human cancer cell line. Moreover, the isolation, structure elucidation, and biological activity of these isolated compounds are reported.



**Citation:** Zhang, J.; Ma, H.; Jin, S.; Liu, X.; Li, L.; Liu, Z.; Li, G.; Li, P. Seven New Lobane Diterpenoids from the Soft Coral *Lobophytum catalai*. *Mar. Drugs* **2023**, *21*, 223. <https://doi.org/10.3390/md21040223>

Received: 6 March 2023

Revised: 29 March 2023

Accepted: 29 March 2023

Published: 30 March 2023



**Copyright:** © 2023 by the authors. Licensee MDPI, Basel, Switzerland. This article is an open access article distributed under the terms and conditions of the Creative Commons Attribution (CC BY) license (<https://creativecommons.org/licenses/by/4.0/>).

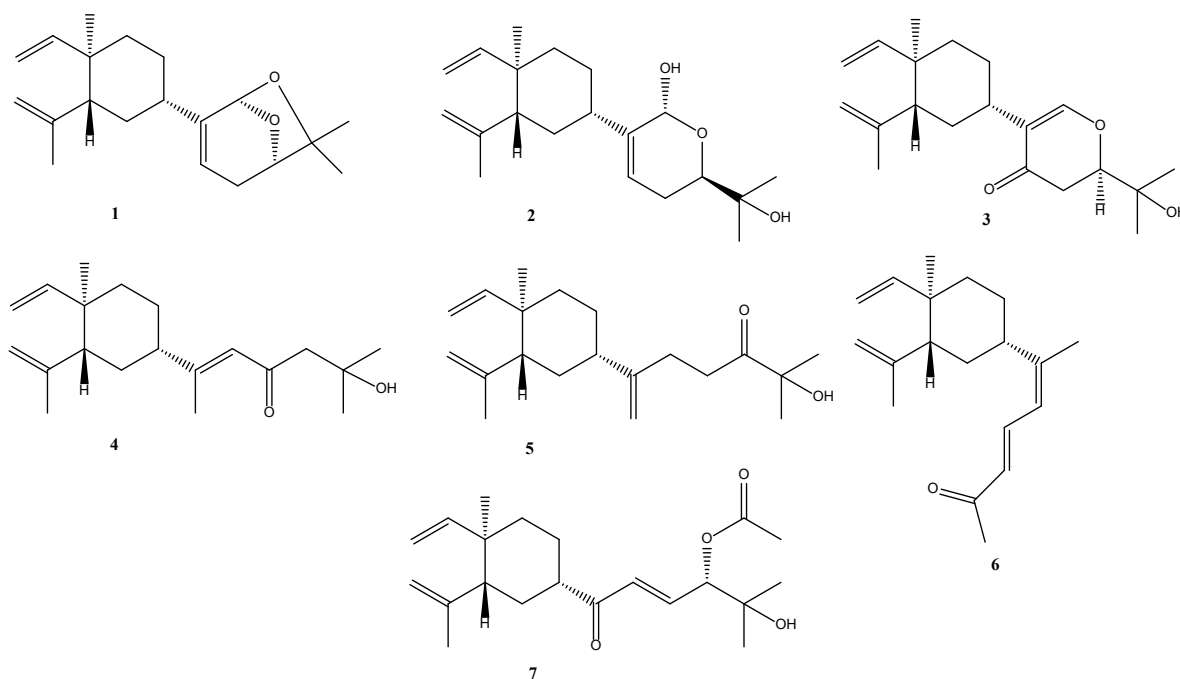


Figure 1. Structures of compounds 1–7.

## 2. Results

Lobocatalen A (1) was isolated as a colorless oil. The HRESIMS experiment exhibited a pseudo-molecular ion peak at  $m/z$  303.2320  $[M + H]^+$ , consistent with the molecular formula of  $C_{20}H_{30}O_2$ , requiring six degrees of unsaturation. The clear IR absorption at 3079 and  $1635\text{ cm}^{-1}$  together with the UV spectrum at  $\lambda_{\text{max}} = 193$  ( $\log \epsilon$  1.65) nm indicated the presence of a double-bond group. The 1D NMR data (Tables 1 and 2) revealed the presence of a monosubstituted terminal double bond (C-9 ( $\delta_C$  110.1,  $CH_2$ ) and C-8 ( $\delta_C$  150.3, CH); H<sub>2</sub>-9 ( $\delta_H$  4.91, d;  $\delta_H$  4.87, s) and H-8 ( $\delta_H$  5.80, dd)), a disubstituted terminal olefinic bond (C-11 ( $\delta_C$  112.4,  $CH_2$ ), C-10 ( $\delta_C$  147.5, CH), and C-12 ( $\delta_C$  24.9,  $CH_3$ ); H<sub>2</sub>-11 ( $\delta_H$  4.81, s;  $\delta_H$  4.57, s) and H<sub>3</sub>-12 ( $\delta_H$  1.69, s)), a ring-junction methyl (C-7 ( $\delta_C$  16.8,  $CH_3$ ); H<sub>3</sub>-7 ( $\delta_H$  0.99, s)), and a ring-junction methine (C-2 ( $\delta_C$  52.7, CH); H-2 ( $\delta_H$  1.99, dd)), which are the characteristic signals of the  $\beta$ -element segment of lobane diterpenoids [4,6,7]. This deduction was then proven by the  $^1H$ - $^1H$  COSY correlations from H-8 to H-9, and from H-2 to H-6, along with the HMBC correlations from H<sub>3</sub>-7 to C-1, C-2, C-6, and C-8, from H<sub>3</sub>-12 to C-2, C-10, and C-11, and from H<sub>2</sub>-15 to C-4 and C-14 (Figure 2).

Table 1.  $^1H$  NMR data of lobocatalens A–G (1–7) ( $CDCl_3$ ).

No.	1	2	3	4	5	6	7
	$\delta_H^a$ (J in Hz)	$\delta_H^b$ (J in Hz)	$\delta_H^b$ (J in Hz)	$\delta_H^b$ (J in Hz)	$\delta_H^a$ (J in Hz)	$\delta_H^a$ (J in Hz)	$\delta_H^b$ (J in Hz)
1							
2	1.99, dd (4.0,12.4)	2.02, m	2.07, dd (3,12.6)	2.01, m	2.01, m	2.12, dd (3.5,12.5)	2.01, dd (4.5,16.5)
3a	1.57, m	1.60, m	1.61, m	1.52, m	1.57, m	1.78, m	1.60, m
3b	1.49, m	1.52, m	1.50, m	1.64, m	1.59, m	1.33, m	1.72, m
4	1.92, m	2.08, m	2.47, m	2.05, m	1.93, m	2.86, m	2.62, m
5a	1.61, m	1.63, m		1.60, m	1.47, m	1.42, m	1.66, m
5b	1.39, m	1.47, m	1.54, m	1.51, m	1.63, m	1.61, m	1.75, m
6a			1.52, m				
6b	1.44, m	1.43, m	1.44, m	1.49, m	1.49, m	1.47, m	1.50, m
7	0.99, s	1.00, s	1.01, s	1.01, s	1.01, s	1.03, s	1.01, s

Table 1. Cont.

No.	1	2	3	4	5	6	7
	$\delta_H^a$ (J in Hz)	$\delta_H^b$ (J in Hz)	$\delta_H^b$ (J in Hz)	$\delta_H^b$ (J in Hz)	$\delta_H^a$ (J in Hz)	$\delta_H^a$ (J in Hz)	$\delta_H^b$ (J in Hz)
8	5.80, dd (10.4,17.6)	5.80, dd (10.8,18)	5.80, dd (10.2,18)	5.81, dd (10.5,17.5)	5.82, dd (10.4,17.6)	5.84, m	5.81, dd (11.5,18)
9a	4.91, d (3.6)	4.91, d (3.2)	4.91, d (4.2)	4.93, d (3.0)	4.93, d (4.4)	4.94, m	4.94, m
9b	4.87, s	4.88, s	4.89, s	4.90, d (2.5)	4.89, s		4.90, m
10							
11a	4.81, s	4.81, s	4.57, s	4.84, s	4.82, s	4.84, s	4.84, s
11b	4.57, s	4.57, s	4.80, s	4.59, s	4.59, s	4.61, s	4.61, s
12	1.69, s	1.70, s	1.69, s	1.71, s	1.71, s	1.73, s	1.71, s
13							
14a	5.36, s	5.48, s	7.27, s	2.17, s	4.84, s	1.90, s	6.34, d (18.0)
14b					4.69, s		
15	5.28, m	5.86, m		6.04, s	2.37, m	5.97, d (11.6)	6.80, m
16a	2.62, d (18.0)	1.97, m	2.45, dd (3,16.8)		2.71, m	7.50, m	5.27, m
16b	2.13, d (4.4,18.4)	2.12, m	2.65, dd (15.6,16.8)				
17	4.19, d (4.8)	3.78, dd (3.6,11.2)	4.11, dd (3.0,15.0)	2.63, s		6.11, dd (4.05,15.4)	
18							1.26, s
19	1.29, s	1.27, s	1.31, s	1.26, s	1.40, s	2.29, s	1.23, s
20	1.36, s	1.23, s	1.24, s	1.26, s	1.40, s		
21							2.15, s

<sup>a</sup> Spectra recorded at 500 MHz. <sup>b</sup> Spectra recorded at 600 MHz.

Table 2. <sup>13</sup>C NMR data of lobocatalens A–G (1–7) (CDCl<sub>3</sub>) <sup>c</sup>.

No.	1	2	3	4	5	6	7
	$\delta_C^d$	$\delta_C^e$	$\delta_C^e$	$\delta_C^d$	$\delta_C^d$	$\delta_C^d$	$\delta_C^d$
1	39.8, C	39.9, C	39.8, C	39.8, C	40.0, C	39.5, C	39.8, C
2	52.7, CH	52.8, CH	52.8, CH	52.6, CH	52.9, CH	52.3, CH	52.1, CH
3	32.8, CH <sub>2</sub>	34.3, CH <sub>2</sub>	34.3, CH <sub>2</sub>	32.4, CH <sub>2</sub>	33.4, CH <sub>2</sub>	32.0, CH <sub>2</sub>	29.5, CH <sub>2</sub>
4	42.3, CH	40.7, CH	34.72, CH	49.4, CH	45.0, CH	41.2, CH	49.6, CH
5	26.4, CH <sub>2</sub>	26.7, CH <sub>2</sub>	26.6, CH <sub>2</sub>	26.4, CH <sub>2</sub>	27.4, CH <sub>2</sub>	26.2, CH <sub>2</sub>	24.0, CH <sub>2</sub>
6	39.8, CH <sub>2</sub>	39.8, CH <sub>2</sub>	40.0, CH <sub>2</sub>	39.7, CH <sub>2</sub>	40.1, CH <sub>2</sub>	39.7, CH <sub>2</sub>	39.2, CH <sub>2</sub>
7	16.8, CH <sub>3</sub>	16.7, CH <sub>3</sub>	16.7, CH <sub>3</sub>	16.8, CH <sub>3</sub>	16.8, CH <sub>3</sub>	16.7, CH <sub>3</sub>	16.6, CH <sub>3</sub>
8	150.3, CH	150.2, CH	150.3, CH	149.8, CH	150.3, CH	150.0, CH	149.8, CH
9	110.1, CH <sub>2</sub>	110.1, CH <sub>2</sub>	110.1, CH <sub>2</sub>	110.4, CH <sub>2</sub>	110.1, CH <sub>2</sub>	110.3, CH <sub>2</sub>	110.5, CH <sub>2</sub>
10	147.5, C	147.6, C	147.5, C	147.3, C	147.7, C	147.3, C	147.0, C
11	112.4, CH <sub>2</sub>	112.4, CH <sub>2</sub>	112.3, CH <sub>2</sub>	112.6, CH <sub>2</sub>	112.4, CH <sub>2</sub>	112.5, CH <sub>2</sub>	112.9, CH <sub>2</sub>
12	24.9, CH <sub>3</sub>	25.0, CH <sub>3</sub>	25.0, CH <sub>3</sub>	25.0, CH <sub>3</sub>	24.9, CH <sub>3</sub>	25.1, CH <sub>3</sub>	24.9, CH <sub>3</sub>
13	146.3, C	137.5, C	122.9, C	164.4, C	153.2, C	155.5, C	202.0, C
14	99.2, CH	101.0, CH	158.8, CH	18.5, CH <sub>3</sub>	107.6, CH <sub>2</sub>	21.1, CH <sub>3</sub>	130.7, CH
15	115.7, CH	124.6, CH	192.3, C	122.5, CH	28.4, CH <sub>2</sub>	124.2, CH	139.5, CH
16	28.0, CH <sub>2</sub>	25.6, CH <sub>2</sub>	37.3, CH <sub>2</sub>	203.0, C	34.4, CH <sub>2</sub>	138.2, CH	79.2, CH

Table 2. Cont.

No.	1	2	3	4	5	6	7
	$\delta_C^d$	$\delta_C^e$	$\delta_C^e$	$\delta_C^d$	$\delta_C^d$	$\delta_C^d$	$\delta_C^d$
17	80.1, CH	73.1, CH	84.8, CH	54.4, CH <sub>2</sub>	214.1, C	128.4, CH	72.3, C
18	81.3, C	72.3, C	71.4, C	70.1, C	76.4, C	199.0, C	26.4, CH <sub>3</sub>
19	29.9, CH <sub>3</sub>	26.4, CH <sub>3</sub>	26.0, CH <sub>3</sub>	29.6, CH <sub>3</sub>	26.8, CH <sub>3</sub>	28.3, CH <sub>3</sub>	25.6, CH <sub>3</sub>
20	24.0, CH <sub>3</sub>	23.5, CH <sub>3</sub>	24.6, CH <sub>3</sub>	29.6, CH <sub>3</sub>	26.8, CH <sub>3</sub>		170.1, C
21							21.2, CH <sub>3</sub>

<sup>c</sup> The assignments were based on HMQC and HMBC spectra. <sup>d</sup> Spectra recorded at 125 MHz. <sup>e</sup> Spectra recorded at 150 MHz.

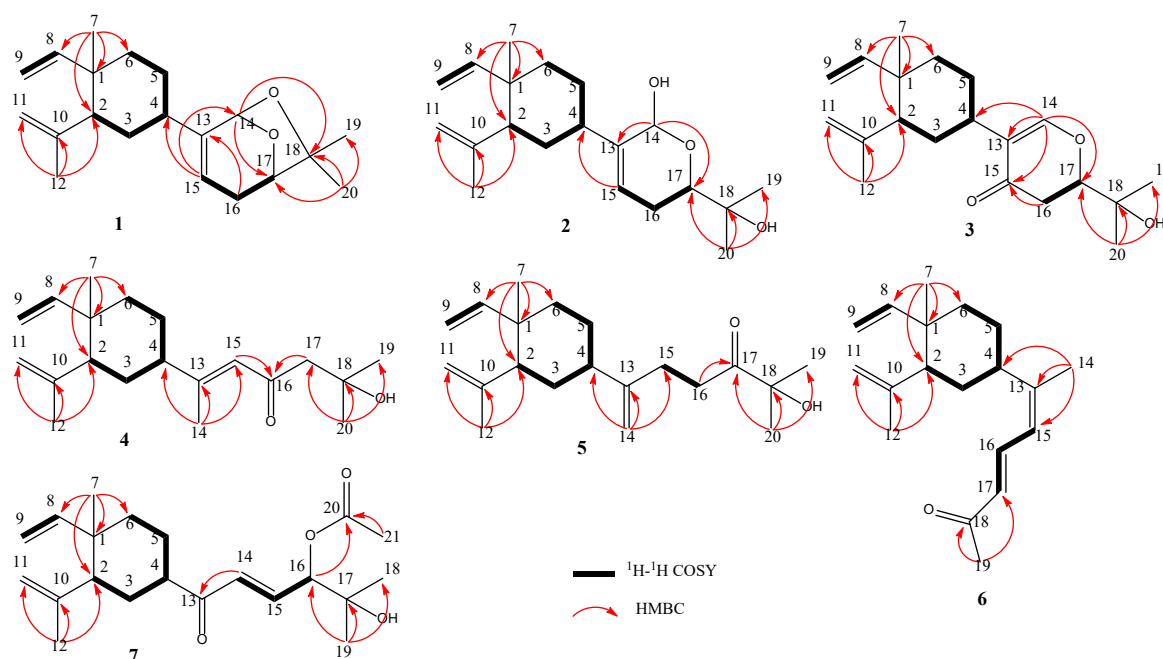
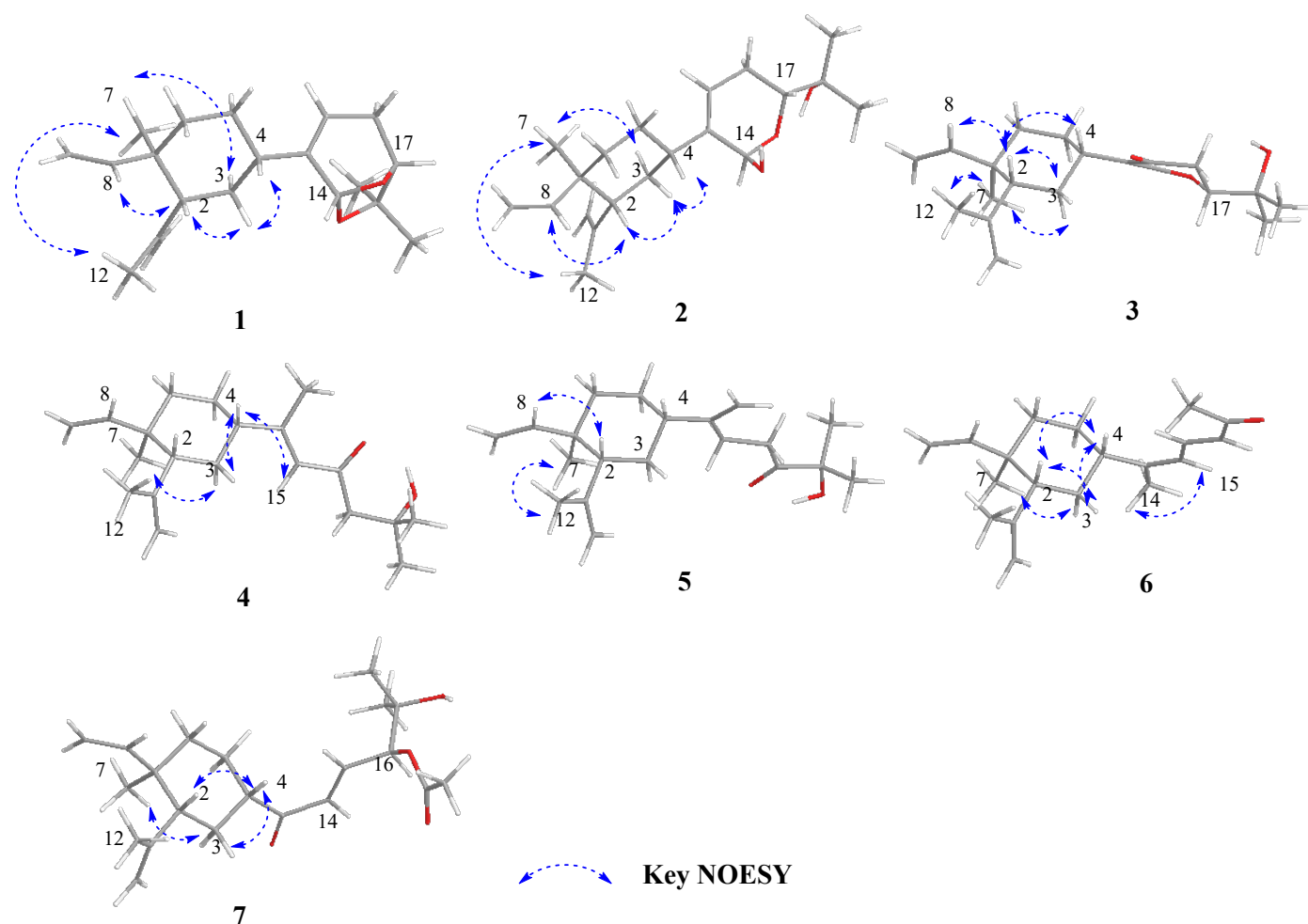


Figure 2. Key <sup>1</sup>H-<sup>1</sup>H COSY and HMBC correlations for compounds 1–7 from *Lobophytum Catalai*.

The remaining two methyls (sp<sup>3</sup>-hybridized), methylene (sp<sup>3</sup>-hybridized), three methines (one olefinic and two oxygenated), and two non-protonated carbons (one oxygenated and one olefinic) are related to the side chain of lobane diterpenoids. Based on the above data, a six-membered ether ring was established based on the <sup>1</sup>H-<sup>1</sup>H COSY correlations from H-15 to H-17, and the HMBC correlations from H<sub>2</sub>-16 to C-13, and from H-14 ( $\delta_H$  5.36, s) to C-17 ( $\delta_C$  80.1) (Figure 2). The above data accounted for five degrees of unsaturation; thus, the remaining degree was designated as a one-ring system. This deduction was further proven by the HMBC correlations from H-14 to C-18, and from H<sub>3</sub>-20 to C-17, C-18 ( $\delta_C$  81.2), and C-19, combined with the significant downfield shifts observed for C-14 ( $\delta_C$  99.2), C-17 ( $\delta_C$  80.1), and C-18 ( $\delta_C$  81.2). Thus, a new lobane diterpenoid (1) with an unusual ether linkage between C-14 and C-18 was established (Figure 2).

In the NOESY spectrum of 1 (Figure 3), the clear correlations of H-3a ( $\delta_H$  1.57)/H-2, H-3a ( $\delta_H$  1.57)/H-4, H-3b ( $\delta_H$  1.49)/H<sub>3</sub>-7, H<sub>3</sub>-7/H<sub>3</sub>-12, and H-2/H-8 indicated the  $\beta$ -orientation of H-2 and H-4, and the  $\alpha$ -orientation of H<sub>3</sub>-7. This deduction was further proven through a comparison of the chemical shifts with previously reported lobane-type diterpenoids [4–7]. The orientations of C-14 and C-17 were defined as 14*R*\* and 17*R*\* in the DP4<sup>+</sup> calculations (Supplementary Materials, Figure S2) [17]. Finally, the absolute configurations of 1 were defined as 1*R*, 2*R*, 4*S*, 14*R*, and 17*R* in the TDDFT-ECD calculations (Figure 4).



**Figure 3.** Key NOESY correlations for compounds 1–7.

Lobocatalen B (**2**) was obtained as a colorless oil. The molecular formula of **2** was determined to be  $C_{20}H_{32}O_3$  based on its HRESIMS ion peak at  $m/z$  338.2685  $[M + NH_4]^+$ . The IR absorption at 3080 and 1635  $cm^{-1}$  together with the UV spectrum at  $\lambda_{max} = 193$  ( $\log \epsilon$  0.38) nm indicated the presence of a double-bond group. Additionally, the IR absorption at 3410  $cm^{-1}$  indicated the presence of a hydroxy group. The 1D NMR data of **2** (Tables 1 and 2) were similar to those of lobatriene [18], a known lobane diterpenoid isolated from an Okinawan soft coral of the genus *Sinularia flexibilis*. The only difference between them is that one hydrogen atom of methylene at C-14 in lobatriene is replaced by a hydroxy group in **2**. The key HMBC correlations (Figure 2) from H-14 ( $\delta_H$  5.48) to C-13 and C-17 and the significant downfield chemical shifts of C-14 ( $\delta_C$  101.1) also supported the change in functional groups. Thus, the planar structure of **2** was constructed (Figure 2). Through a comparison with the NMR data of previously reported lobane-type diterpenoids for which the cyclohexane systems all have the same stereochemistry of  $1R^*$ ,  $2R^*$ , and  $4S^*$  [4–7], the relative configurations of C-1, C-2, and C-4 of **2** were the same as those reported for lobane-type diterpenoids. The NOESY correlations (Figure 3) of H-3a ( $\delta_H$  1.60)/H-2, H-4/H-3a, H-3b ( $\delta_H$  1.52)/H<sub>3</sub>-7, H<sub>3</sub>-7/H<sub>3</sub>-12, and H-2/H-8 further confirmed this deduction. The optical rotation of **2** is  $[\alpha]_D^{25} -40.1$ , which is similar to that of **1** ( $[\alpha]_D^{25} -30.1$ ). Because of the homologous structures, the similar optical rotation data may imply the same relative configuration. The relative configurations of all the asymmetric centers in **2** were established in the DP4<sup>+</sup> calculations (Supplementary Materials, Figure S3). The absolute configurations were further determined as  $1R$ ,  $2R$ ,  $4S$ ,  $14R$ , and  $17R$  in the TDDFT-ECD calculations (Figure 4).

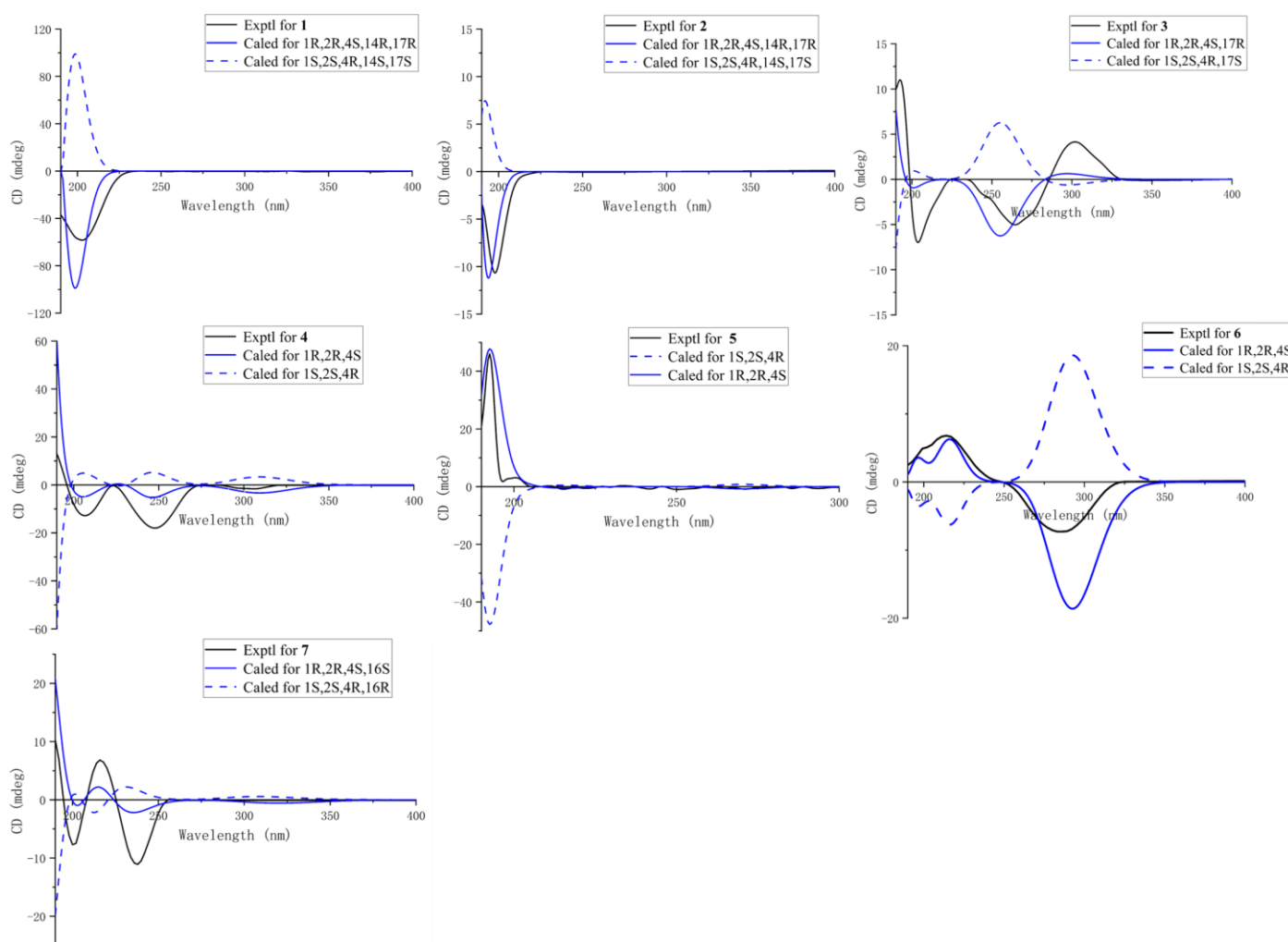


**Figure 4.** Experimental and calculated ECD spectra of compounds 1–7.

Lobocatalen C (**3**), a colorless oil, possesses a molecular formula of  $C_{20}H_{30}O_3$  on the basis of its HREIMS ion peak at  $m/z$  319.2265  $[M + H]^+$ , requiring six degrees of unsaturation. The IR absorption at  $1664\text{ cm}^{-1}$  together with the UV spectrum at  $\lambda_{\text{max}} = 273$  ( $\log \epsilon$  0.12) nm indicated the presence of an  $\alpha$ ,  $\beta$ -unsaturated carbonyl group. The 1D NMR data (Tables 1 and 2) of compound **3** resembled those of lobatrienolide [19], a known lobane diterpenoid isolated from an Okinawan soft coral of the genus *Sinularia flexibilis*. In fact, compound **3** has the same functional groups as lobatrienolide, except for the migration of the double bonds at C-13 and C-15 in lobatrienolide to C-13 and C-14 in **3**, and that of the carbonyl group at the C-14 position in lobatrienolide to C-15 in **3**. This deduction was proven by the key HMBC correlations (Figure 2) from H-14 to C-4, C-13, C-15 ( $\delta_C$  192.3), and C-17 ( $\delta_C$  84.8), and from H-16 to C-15. The  $1R^*$ ,  $2R^*$ , and  $4S^*$  configurations of the  $\beta$ -elemene ring system, which were the same as those of the co-isolates, were determined based on the NOESY correlations (Figure 3) of H-2/H-4, H-2/H-3a ( $\delta_H$  1.61), H-7/H-3b ( $\delta_H$  1.50),  $H_3$ -7/ $H_3$ -12 ( $\delta_H$  1.69), and H-2/H-8, along with the similar chemical shifts of the  $\beta$ -elemene ring system compared with the co-isolates. The relative configuration of C-17 was deduced as  $R^*$  in the DP4<sup>+</sup> calculations (Supplementary Materials, Figure S4). Finally, the absolute configurations of **3** were defined as  $1R$ ,  $2R$ ,  $4S$ , and  $17R$  in the TDDFT-ECD calculations (Figure 4).

Lobocatalen D (**4**) was isolated as a colorless oil. Its molecular formula,  $C_{20}H_{32}O_2$ , was established based on its HRESIMS ion peak at  $m/z$  305.2475  $[M + H]^+$ . The IR absorption at  $1631\text{ cm}^{-1}$  together with the UV spectrum at  $\lambda_{\text{max}} = 271$  ( $\log \epsilon$  0.53) nm indicated the presence of an  $\alpha$ ,  $\beta$ -unsaturated carbonyl group. The 1D NMR data (Tables 1 and 2) of

**4** resembled those of loba-8,10,13(15)-triene-17,18-diol [20], a known lobane diterpenoid isolated from a soft coral of the genus *Lobophytum*. In fact, the structure of **4** is truly similar to that of loba-8,10,13(15)-triene-17,18-diol. The difference between them is that the 17-OH in loba-8,10,13(15)-triene-17,18-diol is replaced by one hydrogen atom of methylene in **4**, and there is a carbonyl group at C-16 in **4** instead of a methylene as in the known compound. Based on the HMBC correlations from H<sub>3</sub>-14 to C-4, C-13, and C-15, from H-15 to C-16 ( $\delta_C$  203.0), from H-17 to C-16, and from H<sub>3</sub>-20 to C-17 ( $\delta_C$  54.4), C-18 ( $\delta_C$  70.1), and C-19, this deduction was proven (Figure 2).

The relative configurations of **4** were determined through an analysis of its NOESY spectrum (Figure 3). The NOESY correlations of H-3a ( $\delta_H$  1.52)/H-4 and H<sub>3</sub>-7/H-3b ( $\delta_H$  1.64) indicated the  $\beta$ -orientation of H-4, and the  $\alpha$ -orientation of H<sub>3</sub>-7. The *E* geometry of the  $\Delta^{13}$  double bonds was established based on the NOESY correlations of H-15/H-4. Through a comparison of the NMR data with those of previously reported (-)- $\beta$ -elemene-type diterpenoids and the co-isolates, the orientation of H-2 was found to be  $\beta$ . Then, the 1*R*\*, 2*R*\*, and 4*S*\* configurations of the  $\beta$ -elemene ring system of **4** were further proven in the DP4<sup>+</sup> calculations (Supplementary Materials, Figure S5). Finally, the absolute configurations of **4** were unambiguously determined in the TDDFT-ECD calculations as 1*R*, 2*R*, and 4*S* (Figure 4).

Lobocatalen E (**5**) has a molecular formula of C<sub>20</sub>H<sub>32</sub>O<sub>2</sub>, as determined by its HRESIMS ion peak at *m/z* 305.2469 [M + H]<sup>+</sup>, suggesting five degrees of unsaturation. The IR absorption at 1711 cm<sup>-1</sup> indicated the presence of a carbonyl group. Analysis of the <sup>1</sup>H and <sup>13</sup>C NMR spectra (Tables 1 and 2) indicated that **5** has a similar functional group to lobovarol G [4], a known lobane diterpenoid isolated from the soft coral *Lobophytum varium*. The only difference is that the 17-OH in lobovarol G is oxidized to a ketonic group in **5**. Furthermore, the HMBC correlations from H-16 to C-17 ( $\delta_C$  214.1) and from H<sub>3</sub>-20 to C-17, C-18 ( $\delta_C$  76.4), and C-19 and the <sup>1</sup>H-<sup>1</sup>H COSY correlations from H-15 to H-16 confirmed this variation in the functional groups (Figure 2). The NOESY correlations (Figure 3) of H<sub>3</sub>-7/H-12 ( $\delta_H$  1.71) and H-2/H-8, along with the similar NMR data compared with the co-isolates, indicated the 1*R*\* and 2*R*\* configurations of the  $\beta$ -elemene ring system. Then, the <sup>13</sup>C NMR chemical shift calculation in the DP4<sup>+</sup> calculations clearly indicated that the relative configuration of C-4 is *S*\*. Hence, the absolute configurations were confirmed as 1*R*, 2*R*, and 4*S* (Supplementary Materials, Figure S6) in the following TDDFT-ECD calculations.

Lobocatalen F (**6**) was isolated as a colorless oil. The HRESIMS ion peak at *m/z* 273.2213 [M + H]<sup>+</sup> of **6** indicated that its molecular formula is C<sub>19</sub>H<sub>28</sub>O, requiring six degrees of unsaturation. The IR absorption at 1706 cm<sup>-1</sup> together with the UV spectrum at  $\lambda_{\max}$  = 287 (log  $\epsilon$  0.18) nm indicated the presence of an  $\alpha$ ,  $\beta$ -unsaturated carbonyl group. A survey of the literature revealed that the 1D NMR data (Tables 1 and 2) of compound **6** were similar to those of 3, 5-heptadien-2-one [21], a known lobane diterpenoid isolated from the soft coral *Lobophytum microlobulatum* from Havellock Island. The 2D NMR of **6** revealed that the planar structure of **6** is identical to that of 3, 5-heptadien-2-one, which suggested that **6** is a stereoisomer of 3, 5-heptadien-2-one. The same relative configurations of the  $\beta$ -elemene ring system were established in the NOESY experiment (Figure 3) of H-7/H-3a ( $\delta_H$  1.78), H-2/H-3b ( $\delta_H$  1.33), H-4/H-3b ( $\delta_H$  1.33), and H-2/H-4. The geometry of the  $\Delta^{16}$  double bonds was designated as an *E*-configuration based on the large coupling constants ( $J_{16,17}$  = 15.4 Hz). The NOESY correlations of H-15/H<sub>3</sub>-14, along with the down-field chemical shift of C-19 ( $\delta_C$  21.1) [22], designated the *Z*-configuration of the  $\Delta^{13}$  double bonds, revealing the only difference between 3, 5-heptadien-2-one and **6**. Then, the 1*R*\*, 2*R*\*, and 4*S*\* configurations of the  $\beta$ -elemene ring system of **6** were further proven in the DP4<sup>+</sup> calculations (Supplementary Materials, Figure S7). Finally, the absolute configurations of **6** were unambiguously determined as 1*R*, 2*R*, and 4*S* in the TDDFT-ECD calculations (Figure 4).

Lobocatalen G (**7**), a colorless oil, possesses the molecular formula C<sub>21</sub>H<sub>32</sub>O<sub>4</sub>, which was established based on the HRESIMS ion peak at *m/z* 371.2192 [M + Na]<sup>+</sup>. The IR absorption at 1700 cm<sup>-1</sup> together with the UV spectrum at  $\lambda_{\max}$  = 270 (log  $\epsilon$  0.03) nm indicated



the presence of an  $\alpha$ ,  $\beta$ -unsaturated carbonyl group. The 1D NMR data (Tables 1 and 2) of **7** closely resembled those of (1*R*\*,2*R*\*,4*S*\*,15*E*)-loba-8,10, 13(14),15(16)-tetraen-17,18-diol-17-acetate, a known lobane diterpenoid isolated from the Bowden Reef soft coral *Simularia* sp. [8]. In fact, the structure of **7** is truly similar to that of the known compound, with the exception that the 1,1-disubstituted double bond at C-13 in the known compound is replaced by a carbonyl group in **7**. This deduction was proven by the  $^1\text{H}$ - $^1\text{H}$  COSY correlations from H-14 to H-16 and the HMBC correlations from H-14 to C-13 ( $\delta_{\text{C}}$  202.0) (Figure 3). Due to the absent HMBC correlations, the connection between C-4 and C-13 was established based on the molecular degrees of unsaturation.

In the NOESY experiment (Figure 3), the correlations of H-2/H-4, H-7/H-3a ( $\delta_{\text{H}}$  1.60), and H-4/H-3b ( $\delta_{\text{H}}$  1.72) established the 1*R*\*, 2*R*\*, and 4*S*\* configurations of the  $\beta$ -elemene ring system. Moreover, the large coupling constants ( $J_{14,15} = 18.0$  Hz) established the *E* geometry of the  $\Delta^{14}$  double bonds. In the relative configuration of C-16 in **7**, the chiral center far away from the  $\beta$ -elemene ring system was difficult to assign in the NOESY experiment. Then, through the  $^{13}\text{C}$  NMR chemical shift calculation in the DP4+ calculations (Supplementary Materials, Figure S8), the relative configuration of C-16 in **7** was deduced as 16*S*\*. Finally, the absolute configurations of **7** were defined as 1*R*, 2*R*, 4*S*, and 16*S* in the TDDFT-ECD calculations (Figure 4).

On account of the fact that research on the anti-inflammatory activity of lobane diterpenoids in zebrafish models has not been reported up to now, we attempted to identify lobane diterpenoids with anti-inflammatory activity in zebrafish models. The anti-inflammatory effect of compounds **1**–**7** was assessed in  $\text{CuSO}_4$ -induced transgenic fluorescent zebrafish.  $\text{CuSO}_4$  can produce an intense acute inflammatory response in the neuromasts and mechanosensorial cells in the lateral line of zebrafish, stimulating the infiltration of macrophages [22,23]. Thus, the number of macrophages surrounding the neuromasts in zebrafish can be observed and counted under a fluorescence microscope. Therefore, the anti-inflammatory activity of these lobane diterpenoids can be evaluated. As shown in Figure 5, compound **7** showed moderate anti-inflammatory activity by alleviating migration and decreasing the number of macrophages surrounding the neuromasts in  $\text{CuSO}_4$ -induced transgenic fluorescent zebrafish. Meanwhile, the other compounds showed no anti-inflammatory activity.

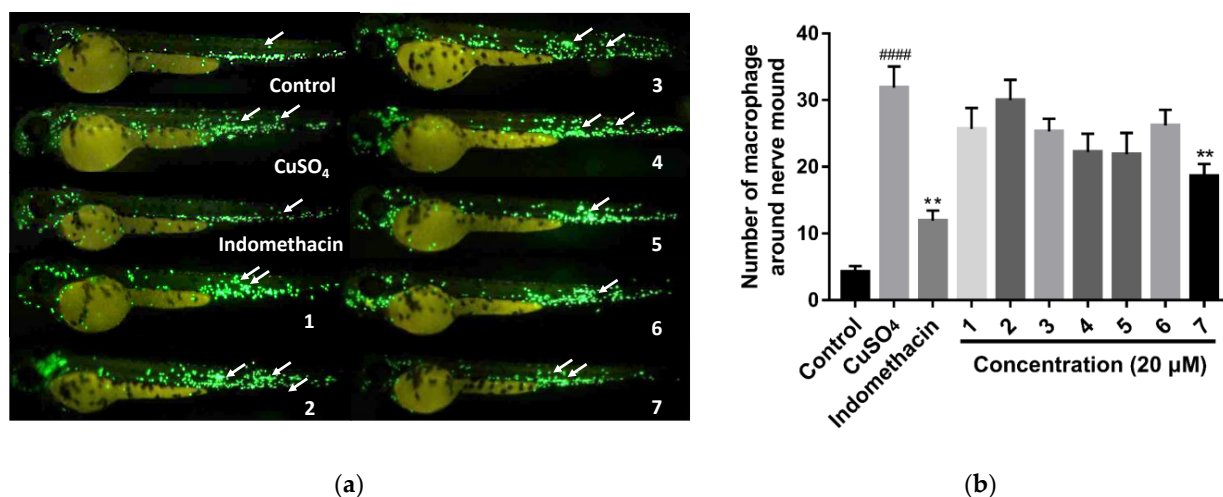


**Figure 5.** Anti-inflammatory assays of compounds **1**–**7**. (a) Images of inflammatory sites in  $\text{CuSO}_4$ -induced transgenic fluorescent zebrafish (Tg: *zlyz*-EGFP) expressing enhanced green fluorescent protein (EGFP) treated with compounds **1**–**7**, using indomethacin as a positive control. (b) Quantitative analysis of macrophages in the region of inflammatory sites in zebrafish treated with compounds **1**–**7** at 20  $\mu\text{M}$ . #### indicates that the  $\text{CuSO}_4$  model group has a very significant difference compared with the control group ( $p < 0.01$ ). \*\* indicates that the sample groups have significant differences compared with the  $\text{CuSO}_4$  model group ( $p < 0.01$ ).



Moreover, the cytotoxic activity of these isolated compounds (1–7) was evaluated against the human leukemia K562, normal human hepatocyte L-02, human pancreatic cancer ASPC-1, and human breast cancer MDA-MB-231 cell lines. The results (Table 3) demonstrated that compound 7 exhibited modest cytotoxicity against the K562 cell line, with an IC<sub>50</sub> value of 27.96 μM.

**Table 3.** Cytotoxic activity (IC<sub>50</sub>, μM) of compounds 1–7.

Compounds	Cell Line			
	K562	L-02	ASPC-1	MDA-MB-231
1	>30	>30	NT <sup>a</sup>	>30
2	>30	>30	NT <sup>a</sup>	>30
3	>30	>30	>30	>30
4	>30	>30	>30	>30
5	>30	NT <sup>a</sup>	NT <sup>a</sup>	NT <sup>a</sup>
6	NT <sup>a</sup>	>30	NT <sup>a</sup>	NT <sup>a</sup>
7	27.96	>30	>30	>30
doxorubicin <sup>b</sup>	<1	<1	<1	<1

<sup>a</sup> NT: not tested. <sup>b</sup> Positive control.

### 3. Materials and Methods

#### 3.1. General Experimental Procedures

Optical rotations were measured using a Jasco P-1020 digital polarimeter (Jasco, Tokyo, Japan). The UV spectra were recorded using a Beckman DU640 spectrophotometer (Beckman Ltd., Shanghai, China). The CD spectra were obtained using a Jasco J-810 spectropolarimeter (Jasco, Tokyo, Japan). The NMR spectra were measured using Agilent 500 MHz (Agilent, Beijing, China) and JEOL JNMECP 600 spectrometers (JEOL, Beijing, China). The 7.26 ppm and 77.16 ppm resonances of CDCl<sub>3</sub> were used as internal references for the <sup>1</sup>H and <sup>13</sup>C NMR spectra, respectively. The HRESIMS spectra were measured using Micromass Q-ToF Ultima GLOBAL GAA076LC mass spectrometers (Autospec-Ultima-TOF, Waters, Shanghai, China). Semi-preparative HPLC was performed using a Waters 1525 pump (Waters, Singapore) equipped with a 2998 photodiode array detector and a YMC C18 column (YMC, 10 × 250 mm, 5 μm). Silica gel (200–300 mesh, 300–400 mesh, and silica gel H, Qingdao Marine Chemical Factory, Qingdao, China) was used for column chromatography.

#### 3.2. Animal Material

The soft coral *Lobophytum catalai* was collected from Xisha Island (YaGong Island) in the South China Sea in 2018 and frozen immediately after collection. The specimen was identified by Ping-Jyun Sung, at the Institute of Marine Biotechnology, the National Museum of Marine Biology and Aquarium, Pingtung 944, Taiwan. The voucher specimen (No. xs-18-yg-113) was deposited at the State Key Laboratory of Marine Drugs, Ocean University of China, People's Republic of China.

#### 3.3. Extraction and Isolation

A frozen specimen of *Lobophytum catalai* (12.0 kg, wet weight) was homogenized and then exhaustively extracted with CH<sub>3</sub>OH six times (5 days each time) at room temperature. The combined solutions were concentrated in vacuo and subsequently desalted by redissolving with ethyl acetate to yield a residue (298.0 g). The crude extract was subjected to silica gel vacuum column chromatography eluted with a gradient of petroleum/ethyl acetate (200:1–1:1, *v/v*) and subsequently eluted with a gradient of CH<sub>2</sub>Cl<sub>2</sub>/MeOH (20:1–1:1, *v/v*) to obtain fourteen fractions (Frs.1–Frs.14). Each fraction was detected via TLC. Frs.3 was subjected to silica gel vacuum column chromatography (petroleum/ethyl acetate, from 20:1 to 1:1, *v/v*) to obtain eight subfractions, Frs.3.1–Frs.3.8. Frs.3.4 was separated via semi-preparative HPLC (ODS, 5 μm, 250 × 10 mm; MeOH/H<sub>2</sub>O, 80:20, *v/v*; 2.0 mL/min) to afford **1** (2.6 mg, t<sub>R</sub> = 82 min). Frs.3.5 was separated via semi-preparative HPLC (ODS,

5  $\mu\text{m}$ , 250  $\times$  10 mm;  $\text{CH}_3\text{CN}/\text{H}_2\text{O}$ , 60:40,  $v/v$ ; 2.0 mL/min) to afford **6** (3.2 mg,  $t_{\text{R}}$  = 70 min). Frs.3.6 was separated via semi-preparative HPLC (ODS, 5  $\mu\text{m}$ , 250  $\times$  10 mm;  $\text{CH}_3\text{CN}/\text{H}_2\text{O}$ , 50:50,  $v/v$ ; 2.0 mL/min) to afford **5** (1.8 mg,  $t_{\text{R}}$  = 110 min). Frs.4 was subjected to silica gel vacuum column chromatography (petroleum/ethyl acetate, 20:1) to obtain six sub-fractions, Frs.4.1–Frs.4.6. Frs.4.6 was separated via semi-preparative HPLC (ODS, 5  $\mu\text{m}$ , 250  $\times$  10 mm;  $\text{CH}_3\text{CN}/\text{H}_2\text{O}$ , 65:35,  $v/v$ ; 2 mL/min) to afford **2** (1.3 mg,  $t_{\text{R}}$  = 70 min) and **3** (2.4 mg,  $t_{\text{R}}$  = 90 min). Frs.5 was subjected to silica gel vacuum column chromatography (petroleum/ethyl acetate, from 20:1 to 1:1,  $v/v$ ) to obtain two subfractions, Frs.6.1–Frs.6.2. Frs.6.1 was separated via semi-preparative HPLC (ODS, 5  $\mu\text{m}$ , 250  $\times$  10 mm;  $\text{MeOH}/\text{H}_2\text{O}$ , 65:35,  $v/v$ ; 2.0 mL/min) to afford **4** (1.8 mg,  $t_{\text{R}}$  = 80 min) and **7** (0.9 mg,  $t_{\text{R}}$  = 121 min).

Lobocatalen A (**1**): colorless oil;  $[\alpha]_{\text{D}}^{25}$   $-30.3$  ( $c$  1.0,  $\text{MeOH}$ ); ECD ( $c$  0.50,  $\text{MeOH}$ ) =  $\Delta\epsilon$ 202  $-58.2$ ; UV ( $\text{MeOH}$ )  $\lambda_{\text{max}}$  ( $\log \epsilon$ ) = 193 (1.65) nm; IR  $\nu_{\text{max}}$  = 3424, 2362, 1635, 1382  $\text{cm}^{-1}$ ; HRESIMS  $m/z$  303.2320  $[\text{M} + \text{H}]^+$  (calcd. for  $\text{C}_{20}\text{H}_{31}\text{O}_2^+$ , 303.2319). For  $^1\text{H}$  NMR and  $^{13}\text{C}$  NMR data, see Tables 1 and 2.

Lobocatalen B (**2**): colorless oil;  $[\alpha]_{\text{D}}^{25}$   $-40.1$  ( $c$  1.0,  $\text{MeOH}$ ); ECD ( $c$  0.50,  $\text{MeOH}$ ) =  $\Delta\epsilon$ 197  $-10.3$ ; UV ( $\text{MeOH}$ )  $\lambda_{\text{max}}$  ( $\log \epsilon$ ) = 193 (0.38) nm; IR  $\nu_{\text{max}}$  = 3410, 2973, 2931, 2360, 1635  $\text{cm}^{-1}$ ; HRESIMS  $m/z$  338.2685  $[\text{M} + \text{NH}_4]^+$  (calcd. for  $\text{C}_{20}\text{H}_{36}\text{O}_3\text{N}^+$ , 338.2685). For  $^1\text{H}$  NMR and  $^{13}\text{C}$  NMR data, see Tables 1 and 2.

Lobocatalen C (**3**): colorless oil;  $[\alpha]_{\text{D}}^{25}$   $-40.3$  ( $c$  1.0,  $\text{MeOH}$ ); ECD ( $c$  0.50,  $\text{MeOH}$ ) =  $\Delta\epsilon$ 192  $+11$ ,  $\Delta\epsilon$ 203  $-6.9$ ,  $\Delta\epsilon$ 265  $-5.1$ ,  $\Delta\epsilon$ 302  $+4.2$ ; UV ( $\text{MeOH}$ )  $\lambda_{\text{max}}$  ( $\log \epsilon$ ) = 193 (0.48), 273 (0.12) nm; IR  $\nu_{\text{max}}$  = 3410, 2972, 2928, 2361, 1664, 1636  $\text{cm}^{-1}$ ; HRESIMS  $m/z$  319.2265  $[\text{M} + \text{H}]^+$  (calcd. for  $\text{C}_{20}\text{H}_{31}\text{O}_3^+$ , 319.2268). For  $^1\text{H}$  NMR and  $^{13}\text{C}$  NMR data, see Tables 1 and 2.

Lobocatalen D (**4**): colorless oil;  $[\alpha]_{\text{D}}^{25}$   $+50.3$  ( $c$  0.5,  $\text{MeOH}$ ); ECD ( $c$  0.50,  $\text{MeOH}$ ) =  $\Delta\epsilon$ 190  $+13.1$ ,  $\Delta\epsilon$ 205  $-12.2$ ,  $\Delta\epsilon$ 248  $-18.8$ ; UV ( $\text{MeOH}$ )  $\lambda_{\text{max}}$  ( $\log \epsilon$ ) = 201 (1.73) nm, 224 (1.63), 271 (0.53) nm; IR  $\nu_{\text{max}}$  = 3431, 2926, 2361, 1631  $\text{cm}^{-1}$ ; HRESIMS  $m/z$  305.2475  $[\text{M} + \text{H}]^+$  (calcd. for  $\text{C}_{20}\text{H}_{33}\text{O}_2^+$ , 305.2475). For  $^1\text{H}$  NMR and  $^{13}\text{C}$  NMR data, see Tables 1 and 2.

Lobocatalen E (**5**): colorless oil;  $[\alpha]_{\text{D}}^{25}$   $+30.7$  ( $c$  1.0,  $\text{MeOH}$ ); ECD ( $c$  0.50,  $\text{MeOH}$ ) =  $\Delta\epsilon$ 193  $+46.6$ ; UV ( $\text{MeOH}$ )  $\lambda_{\text{max}}$  ( $\log \epsilon$ ) = 195 (2.03) nm; IR  $\nu_{\text{max}}$  = 3431, 2928, 2361, 1711, 1634  $\text{cm}^{-1}$ ; HRESIMS  $m/z$  305.2469  $[\text{M} + \text{H}]^+$  (calcd. for  $\text{C}_{20}\text{H}_{33}\text{O}_2^+$ , 305.2475). For  $^1\text{H}$  NMR and  $^{13}\text{C}$  NMR data, see Tables 1 and 2.

Lobocatalen F (**6**): colorless oil;  $[\alpha]_{\text{D}}^{25}$   $-10.4$  ( $c$  1.0,  $\text{MeOH}$ ); ECD ( $c$  0.50,  $\text{MeOH}$ ) =  $\Delta\epsilon$ 199  $+4.9$ ,  $\Delta\epsilon$ 217  $+6.7$ ,  $\Delta\epsilon$ 288  $-7.9$ ; UV ( $\text{MeOH}$ )  $\lambda_{\text{max}}$  ( $\log \epsilon$ ) = 195(1.37), 222(0.66), 287(0.18) nm; IR  $\nu_{\text{max}}$  = 3431, 2927, 2360, 1706, 1558  $\text{cm}^{-1}$ ; HRESIMS  $m/z$  273.2211  $[\text{M} + \text{H}]^+$  (calcd. for  $\text{C}_{19}\text{H}_{29}\text{O}_1^+$ , 273.2213). For  $^1\text{H}$  NMR and  $^{13}\text{C}$  NMR data, see Tables 1 and 2.

Lobocatalen G (**7**): colorless oil;  $[\alpha]_{\text{D}}^{25}$   $-30.5$  ( $c$  0.5,  $\text{MeOH}$ ); ECD ( $c$  0.50,  $\text{MeOH}$ ) =  $\Delta\epsilon$ 191  $+10.3$ ,  $\Delta\epsilon$ 200  $-7.6$ ,  $\Delta\epsilon$ 216  $+6.8$ ,  $\Delta\epsilon$ 238  $-11.1$ ; UV ( $\text{MeOH}$ )  $\lambda_{\text{max}}$  ( $\log \epsilon$ ) = 193 (0.09) nm, 227 (0.12), 270(0.03) nm; IR  $\nu_{\text{max}}$  = 2924, 2854, 1717, 1650, 1540  $\text{cm}^{-1}$ ; HRESIMS  $m/z$  371.2192  $[\text{M} + \text{Na}]^+$  (calcd. for  $\text{C}_{21}\text{H}_{32}\text{O}_4\text{Na}^+$ , 371.2193). For  $^1\text{H}$  NMR and  $^{13}\text{C}$  NMR data, see Tables 1 and 2.

### 3.4. Anti-Inflammatory Activity Assay

Healthy macrophage fluorescent transgenic zebrafish (Tg: zlyz-EGFP) were provided by the Biology Institute of Shandong Academy of Science (Jinan, China). The zebrafish maintenance and anti-inflammation assay were carried out as previously described [24]. Each zebrafish larva was photographed using a fluorescence microscope (AXIO, Zom.V16), and the number of macrophages around the nerve mound was calculated using Image-Pro Plus 6.0 software (Rockville, MD, USA). One-way analysis of variance was conducted using GraphPad Prism 7.00 software (San Diego, CA, USA). Lobocatalens A–G (**1**–**7**) were tested for anti-inflammatory activities in the zebrafish models. Three dpf (days post-fertilization), healthy macrophage fluorescent transgenic zebrafish were used as animal models to evaluate the anti-inflammatory effects of compounds **1**–**7**.

### 3.5. Cytotoxicity Activity Assay

The MTT method was used to evaluate cytotoxicity against the K562 (human leukemia) cell line, and the SRB method was used to evaluate cytotoxicity against the L-02 (normal human hepatocytes), ASPC-1 (human pancreatic cancer), and MDA-MB-231 (human breast cancer) cell lines. As a positive control, Adriamycin (doxorubicin) was used.

## 4. Conclusions

To the best of our knowledge, less than twenty new lobane diterpenoids have been discovered in the last two decades. In our continuing chemical investigation of the Xisha soft coral *Lobophytum catalai*, seven new lobane diterpenoids, named lobocatalens A–G (1–7), were isolated, enriching the chemical diversity of lobane diterpenoids. Among them, lobocatalen A (1) is a new lobane diterpenoid with an unusual ether linkage between C-14 and C-18. Moreover, extensive spectroscopic data analyses, spectral comparisons, quantum chemical calculations, and TDDFT-ECD calculations were combined to determine the structures and absolute configurations of 1–7. In the bioassay, only compound 7 showed moderate anti-inflammatory activity at 20  $\mu$ M in the zebrafish models. This is the first report on the anti-inflammatory activity of lobane diterpenoids in zebrafish. In addition, compound 7 showed modest cytotoxic activity against the K562 human cancer cell line. This research suggests that this species has great potential for further evaluation.

**Supplementary Materials:** The following supporting information can be downloaded at: <https://www.mdpi.com/article/10.3390/md21040223/s1>, Tables S1–S7: NMR data of 1–7; Tables S8–S14 and Figures S2–S8: The determination of relative and absolute configurations for compounds 1–7; Table S15: Anti-inflammation assay of 1–7; Tables S16 and S17: Cytotoxic assay of 1–7; Table S18 and Figures S9–S15: Computational details; Figures S16–S103: Spectra for compounds 1–7.

**Author Contributions:** G.L. and P.L. designed the experiments; J.Z. performed the experiments, isolated the compounds, and analyzed the spectral data; J.Z., S.J., Z.L. and H.M. prepared the Supplementary Materials; L.L. and X.L. performed the anti-inflammatory assay; J.Z. wrote the paper. All authors have read and agreed to the published version of the manuscript.

**Funding:** This work was supported by the National Natural Science Foundation of China (Nos. 81991522, 42276088, U2006204, 41876161).

**Institutional Review Board Statement:** Not applicable.

**Data Availability Statement:** Data are contained within the article or Supplementary Materials.

**Acknowledgments:** Special thanks to the Center for High Performance Computing and System Simulation (Pilot National Laboratory for Marine Science and Technology) for the support extended toward the computer calculations.

**Conflicts of Interest:** The authors declare no conflict of interest.

## References

1. Dunlop, R.W.; Wells, R.J. Isolation of some novel diterpenes from a soft coral of the genus *Lobophytum*. *Aust. J. Chem.* **1979**, *32*, 1345–1351. [[CrossRef](#)]
2. Faulkner, D.J. Marine natural products: Metabolites of marine invertebrates. *Nat. Prod. Rep.* **1984**, *1*, 551–598. [[CrossRef](#)]
3. Gopichand, Y.; Schmitz, F.J. Marine natural products: Fuscol, a new elemene-type diterpene alcohol from the gorgonian *Eunicea fusca*. *Tetrahedron Lett.* **1978**, *19*, 3641–3644. [[CrossRef](#)]
4. Chang, C.-H.; Ahmed, A.F.; Yang, T.-S.; Lin, Y.-C.; Huang, C.-Y.; Hwang, T.-L.; Sheu, J.-H. Isolation of lobane and prenyleudesmane diterpenoids from the soft coral *Lobophytum varium*. *Mar. Drugs* **2020**, *18*, 223. [[CrossRef](#)] [[PubMed](#)]
5. Ye, F.; Chen, Z.-H.; Gu, Y.-C.; Guo, Y.-W.; Li, X.-W. New lobane-type diterpenoids from the Xisha soft coral *Simularia polydactyla*. *Chin. J. Nat. Med. Amst. Neth.* **2020**, *18*, 839–843. [[CrossRef](#)]
6. Ahmed, A.F.; Teng, W.-T.; Huang, C.-Y.; Dai, C.-F.; Hwang, T.-L.; Sheu, J.-H. Anti-Inflammatory lobane and prenyleudesmane diterpenoids from the soft coral *Lobophytum varium*. *Mar. Drugs* **2017**, *15*, 300. [[CrossRef](#)] [[PubMed](#)]
7. Phan, C.-S.; Ng, S.-Y.; Kamada, T.; Vairappan, C.S. Two New Lobane Diterpenes from a Bornean Soft Coral *Simularia* sp. *Nat. Prod. Commun.* **2016**, *11*, 899–900. [[CrossRef](#)]

8. Wright, A.D.; Nielson, J.L.; Tapiolas, D.M.; Liptrot, C.H.; Motti, C.A. A Great Barrier Reef *Sinularia* sp. yields two new cytotoxic diterpenes. *Mar. Drugs* **2012**, *10*, 1619–1630. [[CrossRef](#)]
9. Bonnard, I.; Jhaumeer-Laulloo, S.B.; Bontemps, N.; Banaigs, B.; Aknin, M. New lobane and cembrane diterpenes from two Comorian soft corals. *Mar. Drugs* **2010**, *8*, 359–372. [[CrossRef](#)]
10. Edrada, R.A.; Proksch, P.; Wray, V.; Witte, L.; van Ofwegen, L. Four new bioactive lobane diterpenes of the soft coral *Lobophytum pauciflorum* from Mindoro, Philippines. *J. Nat. Prod.* **1998**, *61*, 358–361. [[CrossRef](#)]
11. Chai, M.C.; Wang, S.K.; Dai, C.F.; Duh, C.Y. A cytotoxic lobane diterpene from the formosan soft coral *Sinularia inelegans*. *J. Nat. Prod.* **2000**, *63*, 843–844. [[CrossRef](#)]
12. Zhang, W.; Krohn, K.; Ding, J.; Miao, Z.-H.; Zhou, X.-H.; Chen, S.-H.; Pescitelli, G.; Salvadori, P.; Kurtan, T.; Guo, Y.-W. Structural and Stereochemical Studies of  $\alpha$ -Methylene- $\gamma$ -lactone-Bearing Cembrane Diterpenoids from a South China Sea Soft Coral *Lobophytum crassum*. *J. Nat. Prod.* **2008**, *71*, 961–966. [[CrossRef](#)] [[PubMed](#)]
13. Cheng, S.-Y.; Wen, Z.-H.; Wang, S.-K.; Chiou, S.-F.; Hsu, C.-H.; Dai, C.-F.; Chiang, M.Y.; Duh, C.-Y. Unprecedented Hemiketal Cembranolides with Anti-inflammatory Activity from the Soft Coral *Lobophytum durum*. *J. Nat. Prod.* **2009**, *72*, 152–155. [[CrossRef](#)] [[PubMed](#)]
14. Duh, C.-Y.; Wang, S.-K.; Huang, B.-T.; Dai, C.-F. Cytotoxic cembrenolide diterpenes from the Formosan soft coral *Lobophytum crassum*. *J. Nat. Prod.* **2000**, *63*, 884–885. [[CrossRef](#)] [[PubMed](#)]
15. Chao, C.-H.; Wen, Z.-H.; Wu, Y.-C.; Yeh, H.-C.; Sheu, J.-H. Cytotoxic and Anti-inflammatory Cembranoids from the Soft Coral *Lobophytum crassum*. *J. Nat. Prod.* **2008**, *71*, 1819–1824. [[CrossRef](#)]
16. Li, L.; Sheng, L.; Wang, C.Y.; Zhou, Y.B.; Huang, H.; Li, X.B.; Li, J.; Mollo, E.; Gavagnin, M.; Guo, Y.W. Diterpenes from the Hainan soft coral *Lobophytum cristatum* Tixier-Durivault. *J. Nat. Prod.* **2011**, *74*, 2089–2094. [[CrossRef](#)] [[PubMed](#)]
17. Suramitr, S.; Piriyaagoon, A.; Wolschann, P.; Hannongbua, S. Theoretical study on the structures and electronic properties of oligo (p-phenylenevinylene) carboxylic acid and its derivatives: Effects of spacer and anchor groups. *Theor. Chem. Acc.* **2012**, *131*, 1209. [[CrossRef](#)]
18. Kusumi, T.; Hamada, T.; Ishitsuka, M.O.; Ohtani, I.; Kakisawa, H. Elucidation of the relative and absolute stereochemistry of lobatriene, a marine diterpene, by a modified Mosher method. *J. Org. Chem.* **1992**, *57*, 1033–1035. [[CrossRef](#)]
19. Hamada, T.; Kusumi, T.; Ishitsuka, M.O.; Kakisawa, H.J.C.L. Structures and Absolute Configurations of New Lobane Diterpenoids from the Okinawan Soft Coral *Sinularia flexibilis*. *Chem. Lett.* **1992**, *21*, 33–36. [[CrossRef](#)]
20. Nagaoka, H.; Iwashima, M.; Miyahara, M.; Yamada, Y. Synthesis of (1R, 2R, 4S, 17R)-LOBA-8, 10, 13(15)-TRIENE-17, 18-DIOL, a Marine Diterpene. *Chem. Pharm. Bull.* **1992**, *40*, 556–558. [[CrossRef](#)]
21. Anjaneyulu, A.S.R.; Rao, N.S.K. Four new lobane diterpenoids from the soft coral *Lobophytum microlobulatum* of the Havellock Island of the Andaman and Nicobar group of islands. *Indian J. Chem.* **1996**, *35*, 1294–1303. [[CrossRef](#)]
22. Wang, C.; Zhang, J.; Shi, X.; Li, K.; Li, F.; Tang, X.; Li, G.; Li, P. Sarcoelegantolides C-G, Five New Cembranes from the South China Sea Soft Coral *Sarcophyton elegans*. *Mar. Drugs* **2022**, *20*, 574. [[CrossRef](#)] [[PubMed](#)]
23. Pereira, T.C.B.; Campos, M.M.; Bogo, M.R. Copper toxicology, oxidative stress and inflammation using zebrafish as experimental model. *J. Appl. Toxicol.* **2016**, *36*, 876–885. [[CrossRef](#)] [[PubMed](#)]
24. Wang, C.L.; Jin, T.Y.; Liu, X.H.; Zhang, J.R.; Shi, X.; Wang, M.F.; Huang, R.; Zhang, Y.; Liu, K.C.; Li, G.Q. Sinudenoids A-E, C (19)-Norcembranoid Diterpenes with Unusual Scaffolds from the Soft Coral *Sinularia densa*. *Org. Lett.* **2022**, *24*, 9007–9011. [[CrossRef](#)] [[PubMed](#)]

**Disclaimer/Publisher’s Note:** The statements, opinions and data contained in all publications are solely those of the individual author(s) and contributor(s) and not of MDPI and/or the editor(s). MDPI and/or the editor(s) disclaim responsibility for any injury to people or property resulting from any ideas, methods, instructions or products referred to in the content.